Full-Wave Analysis of Interconnects in Finite Substrates with Layered Media Formulation of SVS-EFIE for 3D Composite Metal-Dielectric Structures

1st Alireza Niazi
Dept. of ECE
University of Manitoba
Winnipeg, Canada
niazia@myumanitoba.ca

2nd Shucheng Zheng
Dept. of ECE
University of Manitoba
Winnipeg, Canada
shucheng.zheng@umanitoba.ca

3rd Chris Nguyen
Dept. of ECE
University of Manitoba
Winnipeg, Canada
nguye73@myumanitoba.ca

4th Vladimir Okhmatovski
Dept. of ECE
University of Manitoba
Winnipeg, Canada
vladimir.okhmatovski@umanitoba.ca

***Abstract*—In this paper we demonstrate full-wave electromagnetic analysis of the IBM Plasma electronic package nets embedded into the multilayered substrate of finite extent within the framework of a layered medium integral equation formulation. Truncation of the substrate is obtained through inclusion of the finite dielectric regions of air into the otherwise ideal layered medium of the infinite extend. Such air regions introduce the desired effect of physical truncation of the substrate layers, while still allowing for use of integral equation formulations with the layered medium Green's functions avoiding discretization of the layers. Computation framework is based on coupled system of layered medium Mixed Potential Integral Equation (MPIE) and Surface-Volume-Surface Electric Field Integral Equation (SVS-EFIE) suitable for analysis of general composite 3D metal/dielectric structures embedded in layered media.**

***Index Terms*—High-speed interconnects, Electromagnetic modeling, Signal integrity**

I. Introduction

Electromagnetic analysis of interconnect models of electronic packages featuring hundreds of nets, multiple ground/power planes, and tens of dielectric layers sandwiched between them presents a significant challenge for existing computational frameworks. Among most commonly used such frameworks are the ones based on finite element method (FEM) and the method of integral equations (IEs) augmented with layered media Green's functions (LMGF). The Green's functions of the infinite layered substrates are used in the latter in order to confine the unknown field quantities to the surfaces of the metal surfaces (e.g. nets and ground planes) and avoid discretization of the dielectric layer surfaces or volumes. Such LMGF-IE formulations lead to greatly reduced size of the matrix equations compared to the FEM and IE methods based on full discretization of the dielectrics of the substrate as well as the metal components of the package. The major drawback of the LMGF-IE formulations, however, is that they imply the infinite extent of the substrate layers, which unless properly treated do not capture the physical effects associated with truncation of the substrate layers such as reflections of the surface waves, radiation from the substrate edges, and others. To remedy this deficiency of the LMGF-IE frameworks we propose in this work to embed finite volumes of air into otherwise infinitely extended layers described by the LMGF interactions utilized in the IEs. In doing the physical effects due to substrate truncation can be appropriately captured. At the same time discretization of the dielectric layers can be largely avoided except for relatively small volumes of the air regions introduced into the substrate, hence, leading to substantial computational savings.

We enable the LMGF-IE framework through use of coupled system of layered medium MPIEs stated for the metal regions of the interconnects model and SVS-EFIEs for the finite dielectric regions of air introduced into the infinite substrate layers [1]. Such formulation is termed SVS-S-EFIE and is suitable for full-wave electromagnetic analysis of general 3D metal/dielectric composite structures embedded into planar layered media of infinite extent. The layered media electric field Green's functions are formulated and computed in their mixed-potential developed by Michalski, Zhang [2], and Mosig [3] amenable for use in the Method of Moments (MoM) discretization of the SVS-S-EFIE. The MoM discretization of the surfaces of the metal nets and surfaces of the air regions is performed using Rao-Wilton-Glisson basis functions while MoM discretization of the volume polarization currents is performed using tetrahedral meshes with 3 piece-wise constant basis functions introduced for approximation of the polarization current's x-, $y-$, and z-components within each tetrahedron.

The approach is tested on the model of 6 nets from IBM Plasma package [4]. Preliminary results for the computed S-parameters in the models featuring finite and infinite extent dielectric layers are presented in this paper and compared against those computed with commercial electromagnetic analysis tool [5]. Results of further studies on the effectiveness and accuracy of the proposed approach to capturing effects of substrate

979-8-3503-1798-5/23/$31.00 ©2023 IEEE

truncation with LMGF-IEs framework will be demonstrated at the conference.

II. SVS-S-EFIE: Coupled System of SVS-EFIE and MPIE Equations

The SVS-S-V-EFIE formulation ((3) and (4) in [1]) can be stated as the SVS-EFIE formulated for dielectric region $R1$ confined to layer $L2$ ($\boldsymbol{r} \in \partial V_{R1}^{Lp}, \quad p = 2$)

$$\hat{\mathbf{t}}_1(\boldsymbol{r}) \cdot \boldsymbol{E}_{R1}^{Lp}(\boldsymbol{r}) - \hat{\mathbf{t}}_1(\boldsymbol{r}) \cdot \boldsymbol{E}_{Lp}^{\mathrm{sc}}(\boldsymbol{r}) = \hat{\mathbf{t}}_1(\boldsymbol{r}) \cdot \boldsymbol{E}_{Lp}^{\mathrm{inc}}(\boldsymbol{r}), \qquad (1)$$

coupled to MPIE stated for the metal region $R2$ spanning all the P layers

$$-\hat{\mathbf{t}}_2(\boldsymbol{r}) \cdot \boldsymbol{E}_{Lp}^{\mathrm{sc}}(\boldsymbol{r}) = \hat{\mathbf{t}}_2(\boldsymbol{r}) \cdot \boldsymbol{E}_{Lp}^{\mathrm{inc}}(\boldsymbol{r}), \qquad (2)$$

where $\boldsymbol{r} \in \partial V_{R2}^{Lp}, p = 0, ..., P$. In the above couple IEs, $\boldsymbol{E}_{Lp}^{\mathrm{inc}}(\boldsymbol{r})$, $\boldsymbol{E}_{Lp}^{\mathrm{inc}}(\boldsymbol{r})$, and $\boldsymbol{E}_{Lp}^{\mathrm{inc}}(\boldsymbol{r})$ denote incident, scattered, and total electric field at location $\boldsymbol{r}$ in layer Lp. If we represent electric field in terms of vector potential contribution $\boldsymbol{E}_{a,p}^{\mathrm{sc}}(\boldsymbol{r})$ and scalar potential contribution $\boldsymbol{E}_{\nabla\varphi,p}^{\mathrm{sc}}(\boldsymbol{r})$ produced in pth layer by the volumetric polarization current homogeneous region $R1$ as well as vector potential contribution $\boldsymbol{E}_{A,p}^{\mathrm{sc}}(\boldsymbol{r})$ and scalar potential contribution $\boldsymbol{E}_{\nabla\Phi,p}^{\mathrm{sc}}(\boldsymbol{r})$ produced in pth layer by the surface electric current on the surface of metal region $R2$ the above system of 2 coupled IEs becomes

$$\hat{\mathbf{t}}_1(\boldsymbol{r}) \cdot (\boldsymbol{E}_{R1}^{Lp}(\boldsymbol{r}) - [\boldsymbol{E}_{a,p}^{\mathrm{sc}}(\boldsymbol{r}) + \boldsymbol{E}_{\nabla\varphi,p}^{\mathrm{sc}}(\boldsymbol{r})] \qquad (3)$$
$$-[\boldsymbol{E}_{A,p}^{\mathrm{sc}}(\boldsymbol{r}) + \boldsymbol{E}_{\nabla\Phi,p}^{\mathrm{sc}}(\boldsymbol{r})]) = \hat{\mathbf{t}}_1(\boldsymbol{r}) \cdot \boldsymbol{E}_{Lp}^{\mathrm{inc}}(\boldsymbol{r}), \qquad (4)$$
$$\boldsymbol{r} \in \partial V_{R1}^{Lp}, p = 2, \qquad (5)$$
$$\hat{\mathbf{t}}_2(\boldsymbol{r}) \cdot (-[\boldsymbol{E}_{a,p}^{\mathrm{sc}}(\boldsymbol{r}) + \boldsymbol{E}_{\nabla\varphi,p}^{\mathrm{sc}}(\boldsymbol{r})] \qquad (6)$$
$$-[\boldsymbol{E}_{A,p}^{\mathrm{sc}}(\boldsymbol{r}) + \boldsymbol{E}_{\nabla\Phi,p}^{\mathrm{sc}}(\boldsymbol{r})]) = \hat{\mathbf{t}}_2(\boldsymbol{r}) \cdot \boldsymbol{E}_{Lp}^{\mathrm{inc}}(\boldsymbol{r}), \qquad (7)$$
$$\boldsymbol{r} \in \partial V_{R2}^{Lp}, \quad p = 0, ..., P. \qquad (8)$$

The MoM forms linear equations with respect to: a) the vectors of unknown coefficients $\underline{[\mathtt{I}]}$ in the expansion of region $R1$ fictitious surface current $\underline{\mathtt{J}}$ over half-RWG functions; b) the vectors of unknown coefficients $\underline{[I]}$ in the expansion of metal region $R2$ current $\boldsymbol{J}$ over half-RWG functions. Testing the SVS-EFIE (5) with half-RWG functions $\mathsf{B}_p^{m,\jmath}$

$$\left\langle \mathsf{B}_p^{m,\jmath}, \boldsymbol{E}_{R2}^{Lp} \right\rangle - [\langle \mathsf{B}_p^{m,\jmath}, \boldsymbol{E}_{a,p}^{sc} \rangle + \langle \mathsf{B}_p^{m,\jmath}, \boldsymbol{E}_{\nabla\varphi,p}^{sc} \rangle]$$
$$- \left[\langle \mathsf{B}_p^{m,\jmath}, \boldsymbol{E}_{A,p}^{\mathrm{sc}} \rangle + \langle \mathsf{B}_p^{m,\jmath}, \boldsymbol{E}_{\nabla\Phi,p}^{\mathrm{sc}} \rangle\right] = \left\langle \mathsf{B}_p^{m,\jmath}, \boldsymbol{E}_{Lp}^{\mathrm{inc}} \right\rangle, \qquad (9)$$
$$\jmath = 1, 2, 3, \quad p = 2,$$

and testing the MPIE (8) with half-RWG functions $\boldsymbol{B}_p^{m,\jmath}$

$$\left[\langle \boldsymbol{B}_p^{m,\jmath}, \boldsymbol{E}_a^p \rangle + \left\langle \boldsymbol{B}_p^{m,\jmath}, \boldsymbol{E}_{\nabla\varphi}^p \right\rangle\right]$$
$$- [\langle \boldsymbol{B}_p^{m,\jmath}, \boldsymbol{E}_{a,p}^{\mathrm{sc}} \rangle + \langle \boldsymbol{B}_p^{m,\jmath}, \boldsymbol{E}_{\nabla\varphi,p}^{\mathrm{sc}} \rangle] = \left\langle \boldsymbol{B}_p^{m,\jmath}, \boldsymbol{E}_{Lp}^{\mathrm{inc}} \right\rangle, \qquad (10)$$
$$\jmath = 1, 2, 3, \quad p = 0, ..., P.$$

The evaluation of the inner products $\langle \mathsf{B}_p^{m,\jmath}, \boldsymbol{E}_a^p \rangle$, $\langle \mathsf{B}_p^{m,\jmath}, \boldsymbol{E}_{\nabla\varphi}^p \rangle$ performed in exactly the same in the case of layered medium formulation way as it was described in [6] for the case of the free-space SVS-EFIE formulation and is not repeated here. The evaluation of the inner products $\langle \boldsymbol{B}_p^{m,\jmath}, \boldsymbol{E}_{a,p}^{\mathrm{sc}} \rangle$, $\langle \boldsymbol{B}_p^{m,\jmath}, \boldsymbol{E}_{\nabla\varphi,p}^{\mathrm{sc}} \rangle$, $\langle \mathsf{B}_p^{m,\jmath}, \boldsymbol{E}_{a,p}^{\mathrm{sc}} \rangle$, $\langle \mathsf{B}_p^{m,\jmath}, \boldsymbol{E}_{\nabla\varphi,p}^{\mathrm{sc}} \rangle$, $\langle \boldsymbol{B}_p^{m,\jmath}, \boldsymbol{E}_{A,p}^{\mathrm{sc}} \rangle$, $\langle \boldsymbol{B}_p^{m,\jmath}, \boldsymbol{E}_{\nabla\Phi,p}^{\mathrm{sc}} \rangle$, $\langle \mathsf{B}_p^{m,\jmath}, \boldsymbol{E}_{A,p}^{\mathrm{sc}} \rangle$, $\langle \mathsf{B}_p^{m,\jmath}, \boldsymbol{E}_{\nabla\Phi,p}^{\mathrm{sc}} \rangle$ and $\langle \boldsymbol{B}_p^{m,\jmath}, \boldsymbol{E}_{Lp}^{\mathrm{inc}} \rangle$, $\langle \mathsf{B}_p^{m,\jmath}, \boldsymbol{E}_{Lp}^{\mathrm{inc}} \rangle$ involved the dyadic Green's function of the multilayered medium has been discussed in details in [7].

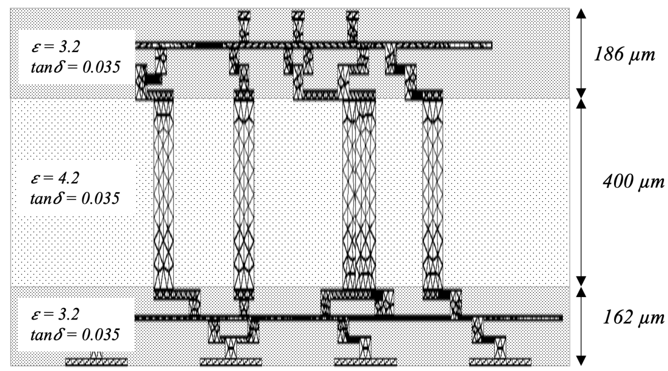

Fig. 1. Configuration of interconnect in three layered medium structure.

III. Numerical Results

To study the finite substrate effects on the signal integrity in package interconnects, we consider 6 nets of the IBM Plasma package [4]. Geometry of the nets is depicted in Figs. 2 and 3. Cross-sectional information about metallization layers and via layers in the package is given in Fig. 1. In the same figure 5-layer dielectric substrate supporting the metal/via layers is shown. For the substrate, the top and bottom layers share the same dielectric material, both having relative permittivity of 3.2 and a loss tangent (delta) of 0.035. These layers are of thickness, measuring 0.186 mm and 0.162 mm, respectively. The middle layer, on the other hand, is made of a different dielectric material with a permittivity of 4.5 and a loss tangent of 0.035. It is thicker than the top and bottom layers, with a thickness of 0.4 mm. The air regions modelled as finite dielectric regions embedded in the substrated are depicted in Fig. 2. Their dimensions are also stated in Table I.

The simulations are conducted using both the StratUM3D academic solver implementing the MoM solution of the layered medium SVS-S-EFIE described in [1] and FEKO commercial solver [5], which also can perform full-wave analysis of composite metal/dielectric structures in layered medium.

In the first scenario, the model involves 6 nets of the package, the surface of which is discretized with 24,628 1st order triangles. This interconnect is embedded in the substrate featuring 5 dielectric layers (Fig. 1) of infinite extent in XY-plane.

In the second scenario, truncation of the substrate is effected by introducing a 1mm wide air gap ring around the interconnect. This air gap was discretized using 8,584 tetrahedral elements, enabling sufficient accuracy of MoM solution. The air gap width was subsequently increased from 1mm to 2mm, in order to monitor whether the width of the air gap is sufficiently large to emulate finite substrate behaviour at all frequencies in the sweep of the S-parameters (from 100MHz to 60GHz). Discretization of the 2mm air gap involved 15,754 tetrahedrons in the MoM discretization of the SVS-S-EFIE, while the number of the triangles involved in discretization of the nets surfaces remained the same (24,628 triangles).

TABLE I
THE CHARACTERISTICS OF THE AIR GAP RING

Ring width	***Inner length***	***Tetrahedron***	***Material***
1 mm	32 mm	8,584	Air
2 mm	32 mm	15,754	Air

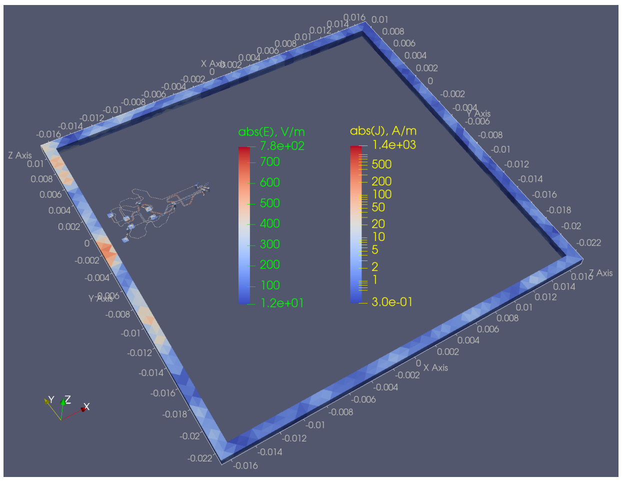

Fig. 2. Magnitude of the total electric field obtained by SVS-EFIE for the interconnect model specifically at a frequency of 40 GHz.

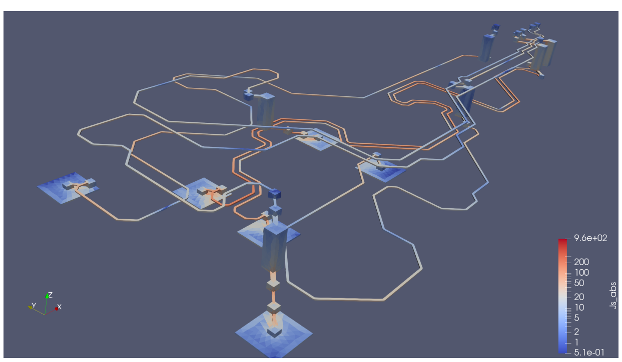

Fig. 3. Magnitude of the total electric field obtained by SVS-EFIE for the interconnect model specifically at a frequency of 40 GHz.

S-parameters computed with SVS-S-EFIE solver and FEKO commercial solver are depicted in Fig. 4 for the case of infinite substrate and the substrate truncated through introduction of the finite air regions. While a notable effect from the substrate truncation is observed at some frequencies (e.g. 27GHz, 42GHz, etc.) further simulations are required for conclusive study of the effectiveness of the proposed computational framework.

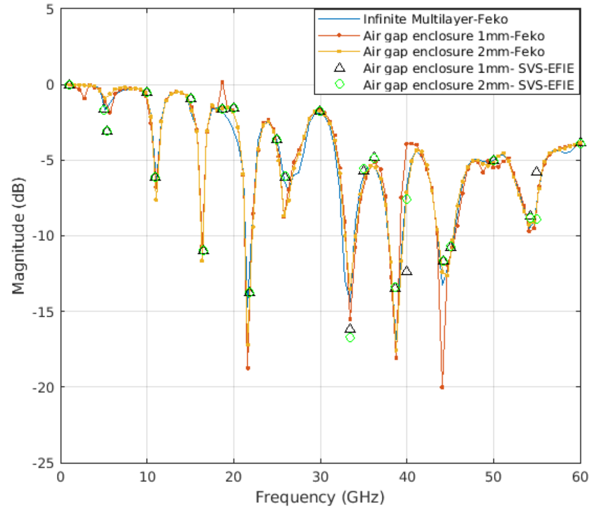

Fig. 4. The S-Parameter results obtained from FEKO and SVS-EFIE simulations cover the frequency range from 1 GHz to 60 GHz.

IV. Conclusion

Paper proposes to computational framework for full-wave analysis of interconnects in finite dielectric substrates based on layered media Green's functions integral equations. In order to truncate the infinite extent of the layers introduced through the use of the layered media Green's functions as the integral equation kernels, finite dielectric regions of air gap are introduced. Handling of these finite size dielectric air regions in conjunction with metal/via layers forming the package nets is enabled via method of moments solution of coupled mixed-potential integral equation and surface-volume-surface electric field integral equation. Proposed approach is tested on the 6 nets of IBM Plasma package from Package Benchmarking Suite.

References

[1] S. Zheng, R. Gholami and V. Okhmatovski, "Surface-Volume-Surface EFIE for Analysis of 3-D Microwave Circuits in Multilayered Substrates With Finite Dielectric Inclusions," 2020 IEEE/MTT-S International Microwave Symposium (IMS), Los Angeles, CA, USA, 2020, pp. 143-145, doi: 10.1109/IMS30576.2020.9223829.

[2] K. A. Michalski and D. Zheng, "Electromagnetic scattering and radiation by surfaces of arbitrary shape in layered media. I. Theory," in IEEE Transactions on Antennas and Propagation, vol. 38, no. 3, pp. 335-344, March 1990, doi: 10.1109/8.52240.

[3] K. A. Michalski and J. R. Mosig, "Multilayered media Green's functions in integral equation formulations," in IEEE Transactions on Antennas and Propagation, vol. 45, no. 3, pp. 508-519, March 1997, doi: 10.1109/8.558666.

[4] IEEE EPS Technical Committee on Electrical Design, Modeling and Simulation, 'Packaging Benchmark Suite', 2021 [Online]. Available: https://packaging-benchmarks.org/.

[5] "FEKO User's Manual," Altair Engineering, 2022.

[6] F. Sheikh Hosseini Lori, A. Menshov, R. Gholami, J. B. Mojolagbe and V. I. Okhmatovski, "Novel Single-Source Surface Integral Equation for Scattering Problems by 3-D Dielectric Objects," in IEEE Transactions on Antennas and Propagation, vol. 66, no. 2, pp. 797-807, Feb. 2018, doi: 10.1109/TAP.2017.2781740.

[7] Zheng, Shucheng. "New single-source surface integral equation for solution of electromagnetic problems in multilayered media." (2022).